POSTER SESSION

THE CRYSTAL STRUCTURE OF rac-N-CARBOXYMETHYLASPARTIC ACID

F. Pavelčík,[1] J. Maderová[1] and J. Marek[2]

[1]Department of Inorganic chemistry, Faculty of Natural Sciences, Comenius University, Mlynská dolina, 842 15 Bratislava, Slovak Republic,
E-mail: maderova@fns.uniba.sk

[2]Department of Inorganic chemistry, Faculty of Natural Sciences, Masaryk University, Kotlářská 2, 611 37, Brno, Czech Republic

The cobalt(III) complexes are not only of interest for their stereochemistry, but also for their application in the bioinorganic field because they provide simple structural models of the metalloprotein active sites. Frequently used ligands are: EDTA, NTA, IPDTA etc.

This work is devoted the synthesis and characterization of N-carboxymethylaspartic acid, (H$_3$cmaa, C$_6$H$_9$NO$_6$). The structure was solved as a part of a general study of the chemistry of aspartic acid derivatives as a ligands in coordination compounds. The title compound is a tetradentate chelating agent that is isomer and chemically similar to nitrilotriacetic acid, but it is chiral.

The H$_3$cmaa was prepared by dissolution of maleic anhydride and glycine in aqueous solution of KOH. The solution was refluxed for 48 h. Then the pH was adjusted by HClO$_4$ to 7 and after filtration the pH was adjusted by HClO$_4$ to 2. The crystals of H$_3$cmaa (**Fig 1**) grew by the slow evaporation of an aqueous solution at 8 °C. After several days obtained colourless crystals were washed by water, ethanol and dried by air.

The crystal data: monoclinic system, P2$_1$/n, a = 5.343(5) Å, b = 16.033(2) Å, c = 9.089(12) Å, β = 95.384(12)°, Z = 4, ρ$_c$ = 1.638 g/cm^3 and contains infinite chains of hydrogen bonds. In the crystal it is not possible to define the organic molecule, because the hydrogen atoms are common for neighbouring molecules.
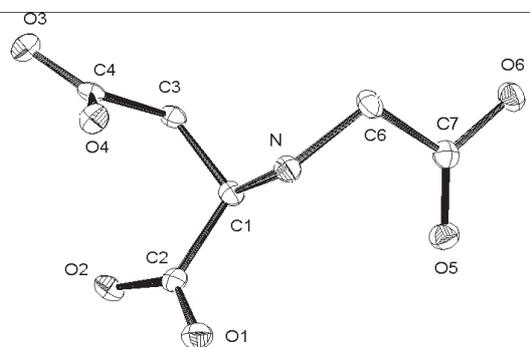

Figure 1. The structure of H$_3$cmaa

CONFORMATION STUDY OF PROLINE RING G IN STRUCTURES OF ERGOPEPTINES

H. Petříčková[1a], M. Hušák[1b], A. Jegorov[2]

[1]Department of Solid State Chemistry, Prague Institute of Chemical Technology, Technická 5, 166 28 Prague 6, Czech Republic,
e-mail: petrickh@vscht.cz[a], husakm@vscht.cz[b]

[2]IVAX CR-Galena Co., Research Unit, Branišovská 31, 370 05 České Budějovice, Czech Republic,
email: alexandr_jegorov@galena.cz

Ergopeptines belong to the large ergot alkaloid family [1]. The ergot alkaloids are produced by parasitic fungi of genus *Claviceps*. Some of their pharmacological effects are known since the Middle Ages. Chemical structure of these substances is close to the structures of natural neurotransmitter [2] (dopamine, adrenaline, serotonine). The ergot alkaloids are used in their natural or chemically modified forms as important drugs. Their most important applications are in the field of treatment of the nerve fibres transport disturbances [3]. They are already used in gynaecology [4], endocrinology, psychiatry, and in treatment of vascular diseases or newly in treatment of obesity [5] as well.

Conformation analysis is relevant for studying interaction between drug and receptor. Not only the chemical structure, but also the conformation of the molecule plays significant role [6]. Molecules of ergopeptines contain four flexible rings C, D, F and G (Fig.1). Flexible central amid bond is fixed by hydrogen bond (O5-H….O1) generally present in all ergopeptines (except ergopeptams).
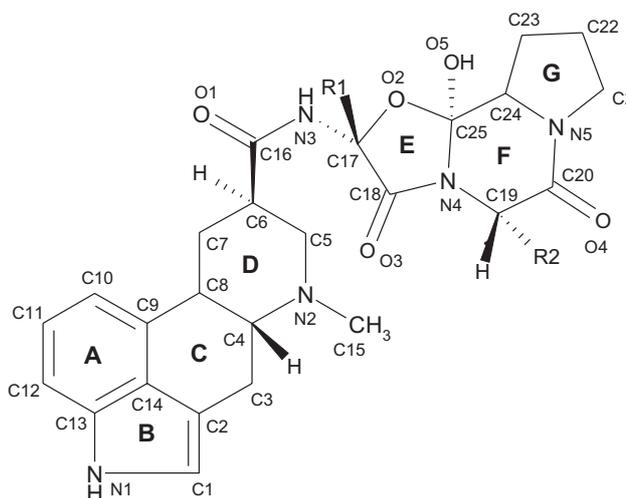

Figure 1. General demonstration of the molecule of ergopeptines with numbering of the atoms and with labeling of the studied rings.

Four new crystal structures of dihydroergopeptines (dihydro-α-ergokryptine methanesulfonate acetone solvate monohydrate (I), dihydro-α-ergokryptine methanesulfonate nitromethan solvate monohydrate (II), dihydro-ergocornine methanesulfonate methanol solvate

monohydrate (III), dihydro-ergocristin methanesulfonate bis(ethyl-acetate) solvate monohydrate) (IV) were solved. Conformation analysis was done for mentioned structures. Ring C has conformation between an envelope form E_3, with C4 atom out of plane of the other five atoms, and half chair $^4H_3$. Ergoline ring D has a stable chair conformation $^4C_1$ with C7 atom above and N2 below the plane of the other four atoms. Stable conformations of ergoline ring D are also fixed by intermolecular hydrogen bonds between hydrogen atoms of protonated N2 and oxygen atoms of methanesulfonate salt. Substituted diketopiperazine ring F adopts an envelope conformation ^6E with C25 atom out of plane of the remaining five atoms. Conformations of the rings C, D and F do not differ from already known eleven structures. The proline ring G assumes most often envelope form ^4E with C23 atom out of plane of the remaining four atoms or twist $^4T_5$ conformation with C23 atom above and C24 below the plane. Two conformations of the proline ring G in newly solved structures I and II significantly differ from those in known ergopeptines: conformation $^1T_2$ - ^1E for I and E_2 - $^3T_2$ for II. Thus, this tempted us to study the proline conformations of all already known ergopeptines. Up to now, no such conformation close to I or II was found.

The molecular dynamics appears suitable for mapping the conformational space of proline. All the proline ring G conformations found in X-ray structures were proved by molecular dynamics.

1. P. W. J.van Dongen, A. N. J. A.de Groot: *Eur. J. Obstetr. Gynecol.*, **60** (1995) 109 - 116.

2. B. Berde & col: *Ergot Compounds and Brain Function: Neuroendocrine and Neuropsychiatric Aspects,* New York 1980. Raven Press.

3. Z. Řeháček, P. Sajdl: *Ergot Alkaloids – Chemistry, Biological Effects and Biotechnology*, Praha 1990. Academia Praha.

4. A. N. J. A de Groot, P. W. J.van Dongen, T. B. Vree, Y. A. Hekster, J. van Roosmalen: Drugs, **56 (4)** (1998) 523 - 535.

5. A. H. Cincotta, A. H. Meier: Diabetes Care, **19 (6)** (1996) 667 - 670.

6. H. P. Weber & col: *Ergot Compounds and Brain Function: Neuroendocrine and Neuropsychiatric Aspects*, New York 1980. Raven Press.

STRUCTURAL STUDIES OF 6-BENZYLAMINOPURINE DERIVATIVES; GROWTH HORMONES WITH ANTI-TUMOR ACTIVITY

M. Maloň[1], J. Marek[2] and Z. Trávníček[1,3]

[1]Department of Inorganic and Physical Chemistry, Faculty of Natural Sciences, Palacký University, CZ-771 47 Olomouc, Czech Republic

[2]X-ray Laboratory of Faculty of Sceinces, Masaryk University, CZ-611 37 Brno, Czech Republic

[3]Laboratory of Growth Regulators, Institute of Experimental Botany ASCR & Palacký University, Šlechtitelů 11, CZ-783 71 Olomouc, Czech Republic
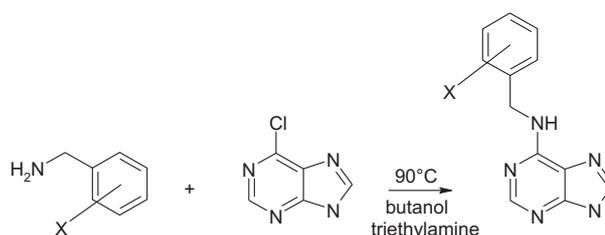
Scheme 1. A representation of preparation of chloro-substituted 6-benzylaminopurine derivatives (X = Cl)

6-Benzylaminopurine derivatives are plant growth hormones and belong to the subgroup of aromatic cytokinins. It was found that some of them have anticancer activity on some animal and human tumours. From this reason, cytokinins and their transition metal complexes are intensively studied. We have found that biological activity of cytokinins can be improved by the complex formation with selected transition metals, mainly Fe^{3+}, Cu^{2+} and Pt^{2+}. To date, we have synthesized, characterized and tested some
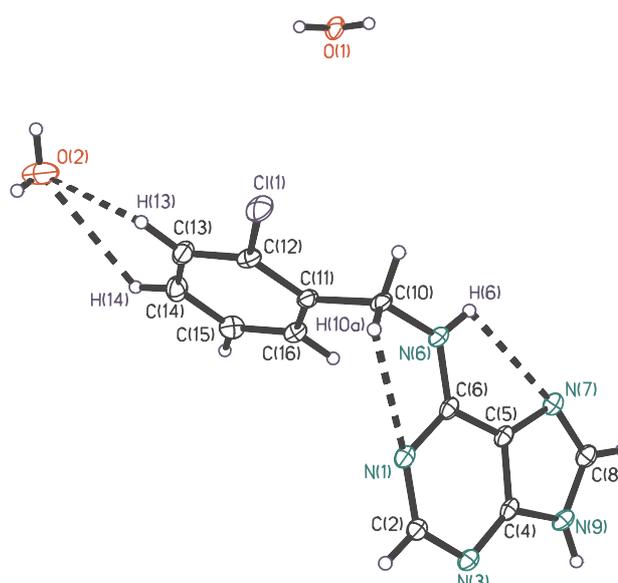

Figure 1. Molecular structure of 6-(2-chlorobenzylamino)purine dihydrate solvate. Thermal ellipsoids are plotted at the 50% probability level. Dashed lines indicate the possible hydrogen bonds. A protonation occurs only on the N(9) atom of purine rings.

transition metal complexes with anti-tumor activity [1-2]. In the present time, we focused our research activities on structural characterization of selected chloro-substituted 6-benzylaminopurine derivatives, namely: 6-(2-chloro-benzylamino)purine, 6-(3-chlorobenzylamino)purine or 6-(4-chlorobenzylamino)purine. The organic compounds have been prepared as depicted in **Scheme 1**. In dependence on pH medium used during the recrystallization, we have obtained the compounds in both an electroneutral (Fig. 1) and protonationed (Figs. 2 and 3) form. Changes in protonation of purine rings have significant influence on differences in some bond lengths and angles.

References

1. Z. Trávníček, M. Maloň, M. Biler, M. Hajdůch, P. Bro□, K. Dole□al, J. Holub, V. Kryštof, & M. Strnad, *Transition Met. Chem.,* **25(3),** 265-269 (2000).

2. Z. Trávníček, M. Maloň, Z. Šindelář, K. Dole□al, J. Rolčík, V. Kryštof, M. Strnad & J. Marek, J. Inorg. Biochem., **84(1-2),** 23-32 (2001).

X-RAY STRUCTURE OF [Cu(N,N-dimeen)(ox)(H₂O)]₂[Cu(N,N-dimeen)₂](ClO₄)₂

J. Kameníček and Z. Smékal

Department of Inorganic and Physical Chemistry, Palacký University, 771 47 Olomouc, Czech Republic

The crystal and molecular structure of the title complex compound (dimeen = N,N-dimethylethylenediamine, ox = oxalate) has been solved by heavy atom methods [1, 2] and basic physico-chemical measurements have been made. It was found that the structure contains two non-equivalent copper atoms in the slightly distorted square-planer (Cu2) and square-pyramidal (Cu1) coordination (see Fig. 1) with deviations of atom positions from square plane smaller then 0.28 Å.

The basic crystallographic data are summarized in Table 1, important bond lengths and angles in Table 2, possible hydrogen bonds according [3] in Table 3.

The results of magnetochemical measurements (μ_{eff} = 1.82 BM/294 K) correspond with assumption of copper in the oxidation state II. The value of molar conductivity (10^{-3} mol/l, in water) χ_M = 307 Scm²mol⁻¹ confirms an electrolyte 1:2 with ClO₄⁻ group out from coordination sphere of the central atoms; the characteristic absorption for this group at 1068 and 620 cm⁻¹ were also found in the IR-spectrum.

References

1. Sheldrick, G.M., SHELXS-97, enhanced version of SHELX-S, *Acta Crystallogr. Sect.A* **46** (1990), 467.

2. Sheldrick, G.M., SHELXL-97, Program for Structure Refinement, University of Göttingen, Germany, 1997.

3. Nardelli, M., PARST-95, *J. Appl. Crystallogr.,* **28** (1995), 659.
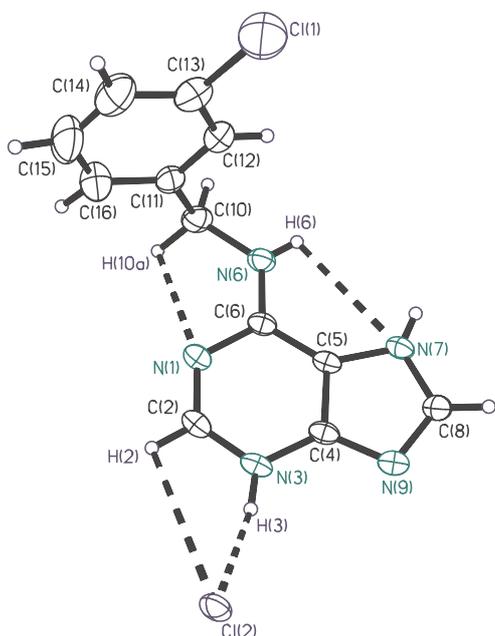

Figure 2. Molecular structure of 6-(3-chlorobenzylami-no)purinium chloride. Thermal ellipsoids are plotted at the 30% probability level. Dashed lines indicate the possible hydrogen bonds. A protonation occurs on the N(3) and N(9) atoms of purine
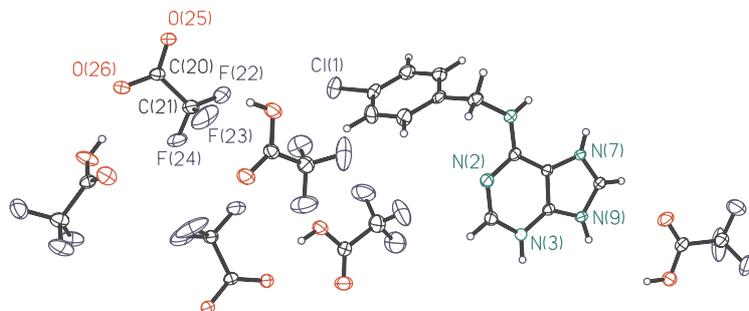

Figure 3. Molecular structure of twice protonationed 6-(4-chlorobenzylamino) purinium trifluoroacetate tetratrifluoroacetic acid solvate. Thermal ellipsoids are plotted at the 50% probability level. A protonation occurs on the N(3), N(7) and N(9) atoms of purine rings.

Table 1. Basic crystallographic data of [Cu(N,N-dimeen)(ox)(H$_2$O)]$_2$ [Cu(N,N-dimeen)$_2$](ClO$_4$)$_2$

|	
Empirical formula	C$_{10}$H$_{26}$ClCu$_{1.5}$N$_4$O$_9$
Formula weight	477.11
Temperature	150(2) K
Wavelength	0.71073 A
Crystal system, space group	Triclinic; P$\bar{1}$
Unit cell dimensions	a = 6.4920(10) Å α = 94.38(3)°
	b = 8.501(2) Å β= 100.68(3)°
	c = 17.079(3) Å γ = 103.80(3)°
Volume	892.3(3) A^3
Z, Calculated density	2; 1.776 Mg/m^3
Absorption coefficient	2.006 mm^{-1}
F(000)	493
Crystal size	0.35 x 0.30 x 0.25 mm
Theta range for data collection	3.67 to 29.21°
Index ranges	-5<=h<=8, -11<=k<=11, -23<=l<=23
Reflections collected / unique	7649 / 4279 [R(int) = 0.0297]
Completeness to 2θ = 29.21	88.5%
Max. and min. transmission	0.6339 and 0.5403
Refinement method	Full-matrix least-squares on F^2
Data / restraints / parameters	4279 / 0 / 258
Goodness-of-fit on F^2	1.080
Final R indices [I>2sigma(I)]	R1 = 0.0431, wR2 = 0.1440
R indices (all data)	R1 = 0.0461, wR2 = 0.1454
Largest diff. peak and hole	0.972 and -0.780 e.A$^-$
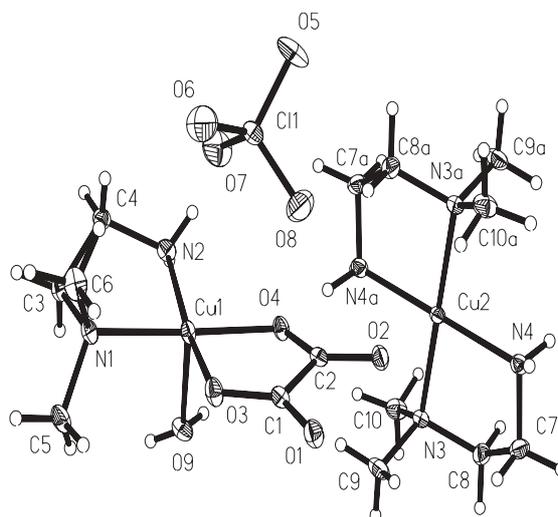
Figure 1
[Cu(N,N-dimeen)(ox)(H$_2$O)]$_2$[Cu(N,N-dimeen)$_2$](ClO$_4$)$_2$
(Cu2 atom is situated in the center of symmetry)

Table 2. Selected bond lengths [Å] and angles [°] for [Cu(N,N-dimeen)(ox)(H$_2$O)]$_2$[Cu(N,N-dimeen)$_2$](ClO$_4$)$_2$

Cu(1)-O(4)	1.940(3)
Cu(1)-O(3)	1.957(3)
Cu(1)-N(2)	2.015(3)
Cu(1)-N(1)	2.022(3)
Cu(1)-O(9)	2.345(3)
Cu(2)-N(4)	1.994(3)
Cu(2)-N(4)#1	1.994(3)
Cu(2)-N(3)#1	2.095(3)
Cu(2)-N(3)	2.095(3)
O(4)-Cu(1)-O(3)	84.50(11)
O(4)-Cu(1)-N(2)	95.18(12)
O(3)-Cu(1)-N(2)	164.41(13)
O(4)-Cu(1)-N(1)	175.16(11)
O(3)-Cu(1)-N(1)	92.57(11)
N(2)-Cu(1)-N(1)	86.61(12)
N(4)-Cu(2)-N(3)#1	94.70(12)
N(4)#1-Cu(2)-N(3)#1	85.30(12)

Table 3. Possible hydrogen bonds for [Cu(N,N-dimeen)(ox)(H$_2$O)]$_2$ [Cu(N,N-dimeen)$_2$](ClO$_4$)$_2$

C3 -H3A	C3 ....O5 (2)	H3A ...O5 (2)	C3 -H3A ...O5 (2)
1.048(.057)	3.517(.032)	2.507(.072)	161.56(.36)
1.080		2.477	161.32
O9 -H9D	O9 ....O5 (2)	H9D ...O5 (2)	O9 -H9D ...O5 (2)
.849(.066)	2.957(.028)	2.136(.060)	162.34(.37)
.938		2.052	161.58
C10 -H10C	C10 ....O2 (6)	H10C...O2 (6)	C10 -H10C...O2 (6)
.960(.113)	3.199(.008)	2.439(.104)	135.84(.33)
1.080		2.355	133.80
N4 -H4C	N4 ....O4 (6)	H4C ...O4 (6)	N4 -H4C ...O4 (6)
.924(.125)	2.893(.034)	2.032(.105)	154.31(.38)
1.030		1.938	152.95
C7 -H7A	C7 ....O8 (5)	H7A ...O8 (5)	C7 -H7A ...O8 (5)
.930(.022)	3.226(.051)	2.484(.041)	136.84(.62)
1.080		2.377	134.37
N4 -H4C	N4 ....O4 (6)	H4C ...O4 (6)	N4 -H4C ...O4 (6)
.924(.125)	2.893(.034)	2.032(.105)	154.31(.38)
1.030		1.938	152.95

IRON(II) AND MAGNESIUM(II) COMPLEXES WITH NON-COORDINATED TRITHIOCYANURIC ACID

P. Kopel[1], J. Marek[2] and Z. Trávníček[1,3]

[1]*Department of Inorganic and Physical Chemistry, Palacký University, Kří□kovského 10, 771 47 Olomouc, Czech Republic*

[2]*X-ray Laboratory of Faculty of Sciences, Masaryk University, Kotlářská 2, 611 37 Brno, Czech Republic*

[3]*Laboratory of Growth Regulators, Institute of Experimental Botany ASCR & Palacký University, Šlechtitelů 11, CZ-783 71 Olomouc, Czech Republic*

Trithiocyanuric acid is well known to form both mononuclear and polynuclear complexes with many metal ions. A manner of its coordination depends not only on the central atom but also on the number and dentacity of the next entering ligands. Some of the structures have been determined by X-ray structure analysis [1-3]. In our previous works we were interested in preparation and study of nickel(II) complexes with trithiocyanuric acid. To date, we have determined five structures of these compounds by a single crystal X-ray analysis [4-6]. The complexes are mononuclear and contain coordinated trithiocyanurate dianion. The coordination number is five or six and the dianion is bonded by N atom or both N and S atoms. We have also prepared nickel complexes with three coordinated bidentate N-donor ligands of the type $[Ni(N-N)_3]$ (ttcH). However, we were not able to obtain suitable single crystals. In the present work we have focused our attention on preparation and structural characterization of complexes with trithiocyanuric acid situated outside of the coordination sphere of the central atom. We have synthesized and structurally characterized the following complexes: $[Fe(bpy)_3](ttcH_2)_2.0,5bpy.EtOH.2H_2O$ **(1)**, $[Fe(phen)_3]$ $(ttcH_2)(ClO_4)$ **(2)** and $[Mg(phen)_3](ttcH_2)_2$ **(3)**, where *ttcH₃* = trithiocyanuric acid, *phen* = 1,10-phenanthroline, *bpy* = 2,2´-bipyridyl.

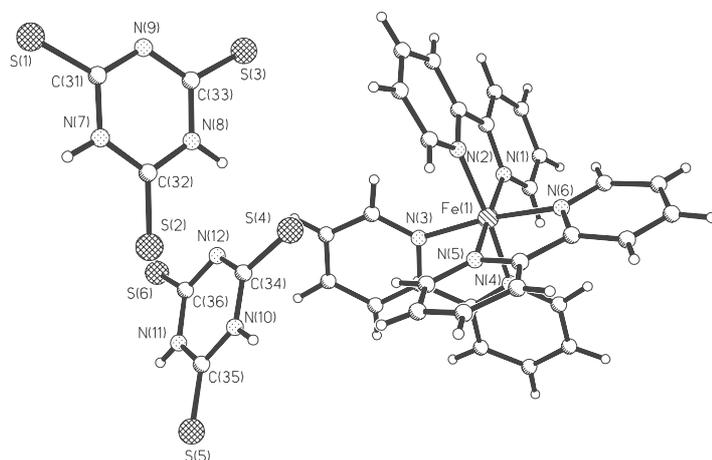1. E.W. Ainscough, A.M. Brodie, R.K. Coll, A.J.A. Mair & J.M. Waters, *Inorg. Chim. Acta,* **214**, (1993) 21.
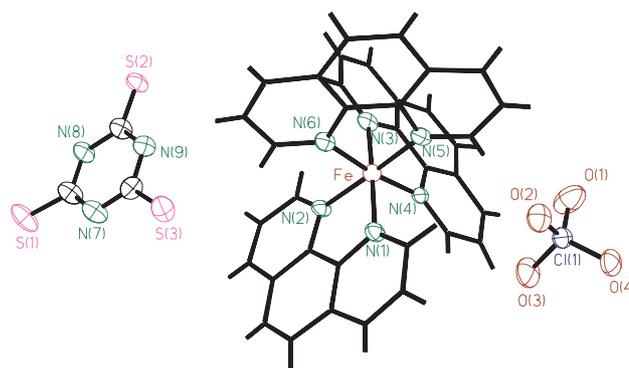
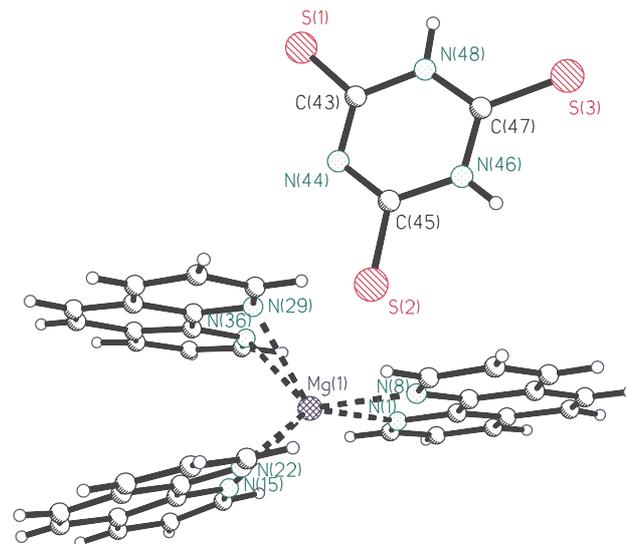**Figure 2**. Molecular structure of **(2)**

Figure 3. Molecular structure of **(3)**

2. C.K. Chan, K.K. Cheung & C.M. Che, *Chem. Comm.,* (1996) 227.

3. B.C. Tzeng, C.M. Che & S.M. Peng, *Chem. Comm.,* (1997) 1771.

4. P. Kopel, Z. Trávníček, R. Panchártková, Z. Šindelář & J. Marek, *J. Coord. Chem*., **44**, (1998) 205.

5. P. Kopel, Z. Trávníček, L. Kvítek, R. Panchártková, M. Biler, J. Marek & M. Nádvorník, *Polyhedron,* **18**, (1999) 1779.

6. P. Kopel, Z. Trávníček, L. Kvítek, M. Biler M. Pavlíček, Z. Šindelář & J. Marek, *Transition Met. Chem*., **26**, (2001) 282.

Figure 1. Molecular structure of **(1)**

DESCRIPTION AND CRYSTAL STRUCTURE OF VAJDAKITE, [(MO^{+6}O$_2$)$_2$(H$_2$O)$_2$ As^{+3}$_2$O$_5$] . H$_2$O – A NEW MINERAL FROM JÁCHYMOV, CZECH REPUBLIC

Petr Ondruš[1], Roman Skála[1], Ivana Císařová[2], František Veselovský[1], Jiří Frýda[1], and Jiří Čejka[3]

[1]*Czech Geological Survey, Klárov 3/131, P.O. Box 85, CZ-118 21 Prague 1, Czech Republic,*

[2]*Faculty of Science, Charles University, Hlavova 2030, CZ-128 43 Prague 2, Czech Republic,*

[3]*National Museum, Václavské nám. 68, CZ-115 79 Prague 1, Czech Republic.*

Vajdakite, a new mineral from Jáchymov, NW Bohemia, Czech Republic, forms minute acicular gray-green crystals associated with arsenolite, scorodite, parascorodite, kaňkite, annabergite, köttigite, pyrite, marcasite, nickelskutterudite, and löllingite. Microprobe analysis gave (wt%): As 27.72, Mo 35.39, O 36.66, totaling 99.77. The simplified chemical formula is [(Mo^{6+}O$_2$)$_2$(H$_2$O)$_2$ As^{3+}$_2$O$_5$] . H$_2$O. The mineral is monoclinic, $P2_1/c$, a = 7.0515(6), b = 12.0908(9), c = 12.2190(14) Å, β = 101.268(9)°, V = 1021.7(2) Å^3, Z = 4, D$_{meas}$ = 3.50(2) g/cm^3, and D$_{calc}$ = 3.509 g/cm^3. The strongest lines in the X-ray powder diffraction pattern d(I)(*hkl*) are: 6.046 (100)(020), 3.324 (59)(023), 6.915 (26)(100), 2.264 (19)(310), 3.457 (16)(200), 2.624 (230), 3.819 (10)(031). Optically positive, X || b, Z/c = 12°, elongation positive, birefrigence is 0.28, 2V$_{calc}$ = 35.1°, α = 1.757(2)°, β = 1.778(2°), γ = 2.04(1)°, pleochroism in X ~ Y light greenish gray, in Z yellowish gray. Crystal size varies between 0.1 to 0.5 mm. TG curve and IR spectra show that vajdakite contains two distinct types of water molecules. The crystal structure was solved by direct methods (MoKα radiation) and refined using 1787 unique reflections to R = 0.0455, Rw = 0.1143. There are double-chains built up by two individual chains with a sequence -O-As-O-Mo- interconnected by oxygens of two
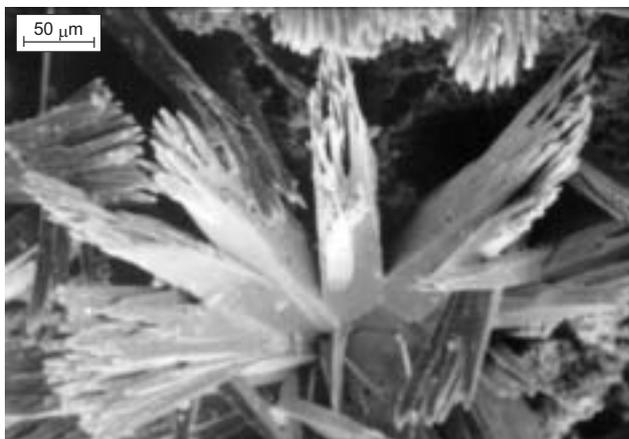

Figure 1. Scanning electron microscope photograph of aggregate of vajdakite acicular crystals. Note crystals termination, which is highly irregular with radiating parallel organized needle-like features. Scale bar corresponds to 50 μm.

triangles AsO$_3$ and two structurally non-equivalent MoO$_5$(H$_2$O) octahedra. Two vertex-sharing triangles of AsO$_3$ form an (As$_2$O$_5$)$^{4-}$ diarsenite group. Two distinct types of water molecules occur in the structure, the first is not included in the coordination, the second one is in octahedral coordination around Mo. They are linked by a complicated net of interlayer and intralayer hydrogen bonds.

CALCULATED X-RAY POWDER DIFFRACTION PATTERNS FOR ZEOLITE-GROUP MINERALS FROM SLOVAKIA

A. Holocsy, P. Fejdi, E. Šamajová[1]

Katedra mineralógie a petrológie, [1]Geologický ústav, Prírodovedecká fakulta UK, Mlynská dolina, 842 15, Bratislava

Calculated X-ray powder diffraction patterns as possible reference data for identification of analcime, garronite, gismondine, harmotome, heulandite, chabazite, klinoptilolite, laumontite, mezolite, mordenite, natrolite, phillipsite, skolecite, stilbite and thomsonite. Calculation procedure were those presented by Kraus and Nolze (1997), input data were coming from original crystal structure refinements. Results are presented in tabular (2θ, interplanar distances d, diffraction indices *h*, *k*, *l* and relative intensities) as well as in pictorial form.

TEXTURES OF ALUMINIUM ALLOY THIN SHEETS FOR HEAT EXCHANGER FINS

J. Marek[1], M. Karlík[2], P. Sláma[3]

[1]*Department of Solid State, Faculty of Nuclear Sciences and Physical, Engineering, Czech Technical University in Prague, Trojanova 13, 120 00 Prague 2, Czech Republic, V Holešovickách 2, 180 00 Praha 8, marek@troja.fjfi.cvut.cz*

[2]*Department of Materials*

[3]*Research Institute for Metals Ltd., Panenské Bre□any, 250 70 Odolena Voda*

Texture analysis of different sheets from Al$_{1.5}$FeMnSi (AA 8006) and AlFeSi (AA 8011) alloys was carried out in order to compare textures of materials for heat exchangers fabricated by several producers and by different technologies. The textures were determined by X-ray back reflection goniometric method using SIEMENS diffractometer. A majority of samples exhibit recrystallization *R*-texture, remaining sheets have a cubic texture or a combination of both texture types. Several samples, fabricated by different technologies, have a texture of the same type. Consequently it is not possible to predict the type of the texture from the technology of casting and downstream processing.

POSITRON-LIFETIME INVESTIGATIONS OF PRECIPITATION EFFECTS IN AL-Cu ALLOY

O. Melikhova[1], J. Čížek[1], I. Procházka[1], J. Kuriplach[1], I. Stulíková[1] and J. Faltus[2]

[1]*Department of Low-Temperature Physics, Faculty of Mathematics and Physics, Charles University, V Holešovičkách 2, CZ-18000, Praha 8, Czech Republic*

[2] *Research Institute of Metals, Panenské Bře□any 50, 250 70 Odolena Voda, Czech Republic.*

The development of new workable aluminium-based alloys is one of the topics in current material science of light alloys. Most of wrought aluminium alloys are based on Al-Cu alloy. Also due to these reasons, there was heavy effort to characterize in details precipitation effects in Al-Cu system. The precipitation effects lead to significant hardening, which improves mechanical properties of Al-Cu based alloys. On the base of a number of investigations [1] performed by various techniques, the following decomposition sequence of Al-Cu system was established:

Supersaturated Solid Solution (SSS) $\Rightarrow$

GP zones $\Rightarrow \theta' \Rightarrow \theta$.

Precipitation starts from the formation of GP zones, which may be regarded as fully coherent metastable particles. With increasing temperature GP zones are replaced by more stable semicoherent precipitates of θ'phase and finally by incoherent precipitates of equilibrium θ phase. Although known for more than 50 years, GP zones in Al-Cu alloys still attract much interest because definitive conclusions on their structure, formation and evolution have not been reached, see [2] and references therein.

Positron lifetime spectroscopy represents well-developed non-destructive and non-local experimental technique for characterisations of microstructure [3]. PL spectroscopy is very sensitive to open volume defects such as vacancies, vacancy clusters, dislocations, grain boundaries, etc. Moreover, under some conditions positrons may be trapped also in precipitates. Lifetime of trapped positrons gets information about kind of defect, while from relative fraction of trapped positrons one can determine concentration of defects. PL spectroscopy is, therefore, ideal tool for investigation of precipitation effects as was proved also in this work on Al-Cu alloy.

The investigated Al-2.0 at.% Cu alloy was firstly homogenized at 525 ^{o}C for 30 min to obtain solid solution. Homogenization was finished by rapid quenching and PL measurement at room temperature. After characterisation of microstructure of as-quenched (AQ) state, the specimen was subjected to isochronal annealing with effective heating rate 1 K/min. Each annealing step was finished by rapid quenching and PL measurements at room temperature.

Two exponential components was found in PL spectrum of AQ specimen: contribution of positrons trapped at quenched-in vacancies associated with Cu atoms (204.9 $\pm$ 0.4 ps, 97.3 $\pm$ 0.2 %) and contribution of positrons trapped in large vacancy clusters (voids) with diameter above 10 nm (570 $\pm$ 20 ps, 2.7 $\pm$ 0.1 %). It was found that the AQ microstructure is stable at room temperature at least in time scale of 50 hours.

PL spectra of the Al-Cu specimen were well fitted by two exponential components (lifetimes τ_1, τ_2) for all annealing temperatures. The first component with lifetime τ_1 comes from free positrons, while the second one with lifetime τ_2 represents contribution of positrons trapped at defects. The lifetime τ_2 lies between the lifetime 180 ps for Cu monovacancy [4] and 250 ps for Al monovacancy [4]. Thus, the component τ_2 is contribution of positrons trapped at vacancies associated with Cu atoms. The decrease of τ_2 with increasing temperature up to 240 ^{o}C is caused by increase of number of Cu atoms in vicinity of vacancy. At temperature 240 ^{o}C the quenched-in vacancies are surrounded exclusively by Cu atoms, which is reflected by τ_2 $\approx$ 180 ps. Concentration of quenched-in vacancies was calculated in the present work as a function of annealing temperature.

Formation of semicoherent θ' precipitates takes place from 260 ^{o}C. Positrons are trapped at misfit defects associated with the θ' particles or directly inside the θ' precipitates. Precipitation of θ' phase causes slight increase of lifetime τ_2, as well as noticeable increase of relative intensity I_2 in temperature region 240-350 ^{o}C. Phase transformation of θ' to θ starts at temperature 320 ^{o}C. In this temperature interval incoherent spherical precipitates of equilibrium θ phase (Al_2Cu) are formed. It is reflected by remarkable increase of lifetime τ_2 to $\approx$ 250 ps. As θ precipitates are incoherent with Al matrix, positrons are trapped at precipitate-matrix interface. Above 400 ^{o}C dissolution of θ precipitates starts. The dissolution of θ precipitates is reflected by radical decrease of relative intensity I_2 in our PL spectra. Clearly, it is due to decreasing number of positron traps at θ precipitate-matrix interfaces. On the other hand, lifetime τ_2 of trapped positrons remains unchanged because there is no change of type of traps.

Theoretical calculations of positron lifetimes and affinities for θ' and θ precipitates were performed in the present work using LMTO technique [5]. It was found that θ precipitates do not represent attractive sites for positrons. Therefore, positrons are trapped at precipitate-matrix interface of incoherent θ precipitates. On the other hand, the θ' precipitates represent attractive sites for positrons. Lifetime of positrons trapped inside the θ' phase particles is 174 ps, i.e. close to the experimental lifetime of trapped positrons in temperature region when θ' phase is present in the specimen. Thus, in the case of θ' precipitates, positrons are trapped at misfit defects introduced into the specimen due to formation of the θ' precipitates and/or directly inside the θ' precipitates.

It was shown in the present work that PL spectroscopy represents powerful tool for investigation of microstructure evolution connected with decomposition of supersaturated solid solution and precipitation effects. Particularly, valuable information about lattice defects and their local chemical surrounding is obtained.

References:

[1] R. Schülbe & U. Schmidt, *phys. stat.sol.*, **(a) 103** (1987) 29. J.M. Silcock, T.J. Heal & H.K. Hardy, *J. Inst. Met.*, **82** (1954) 239. V.A. Phillips, *Acta Met.*, **23** (1973) 751.

[2] M. Karlík & B. Joufrey, *Acta mater.*, **45** (1997) 3251.

[3] P Hautojärvi & Ń. Corbel, in: *Proceedings of The International School of Physics 'Enrico Fermi'* Course CXXV, eds. A. Dupasquier, A.P. Mills, IOS Press, Amsterdam 1995, p. 491.

[4] A. Seeger & F. Banhart, *phys. stat. sol.*, **(a) 102** (1987) 171.

[5] M.J. Puska & R.M. Nieminen, *Rev. Mod. Phys.,* **66** (1994) 841.O.K. Andersen, O. Jepsen & M. Šob, in: *Electronic Band Structure and Its Applications*, ed. M. Yussouff, Springer Verlag, Heidelberg, 1987, p.1.

COCRYSTALLIZATION BEHAVIOUR OF LOW-MOLECULAR-WEIGHT PEO FRACTIONS IN POLYMER BLENDS

J. Baldrian[1], M. Horký[2], M. Steinhart[1], A. Sikora[1], M. Mihailova[3] H. Amenitsch[4], S. Bernstorff[5]

[1]*Institute of Macromolecular Chemistry, Academy of Sciences of the Czech Republic, Heyrovsky Sq.2, 162 06 Prague, Czech Republic*

[2]*Faculty of Nuclear Sciences and Physical Engineering, Czech Technical University, V Holešovičkách 2, 180 00 Prague 8, Czech Republic*

[3]*Faculty of Physics, University of Sofia, J.Bourchier 5, 1126 Sofia, Bulgaria*

[4]*Institute of Biophysics and X-ray Structure Research, Austrian Academy of Sciences, Steyergasse 17, 8010 Graz, Austria*

[5]*Sincrotrone Trieste, Basovizza, 34012 Trieste, Italy*

The aim of this study was to assess the real-time development of poly(ethylene oxide) (PEO) cocrystalline structures in two different kinds of binary blends and thus to contribute to a deeper knowledge of the behaviour of these systems. The time-resolved SAXS/WAXS method on synchrotron and time-modulated DSC were used in this study.

Blends of PEO (3000) and PEO (4000) were studied during isothermal crystallization and during cooling and heating. A single cocrystal system or this system with a small amount of another lamellar systems are formed in the blends during both treatments. The thickness of the cocrystal lamellae depends on the composition of blends, crystallization temperature and grows with growing concentration of PEO (4000) in blends. This thickening is caused by a growing number of higher-molecular-weight chains incorporated in cocrystal lamellae. Small amount of the original cocrystals recrystallize during thermal treatment to the 1F and EC structures probably consisting of neat PEO (3000). During heating, upon approaching the melting points of the respective components, all blend structures recrystallize in the bulk volume giving a new, single and more stable cocrystal structure.

Binary mixtures of PEO (3000) or PEO (4000) with triblock copolymer PEO-*block*-PPO-*block*-PEO were studied. In the neat copolymer and in blends with predominating copolymer two different lamellar systems LP1 (with thicker lamellae) and LP2 are simultaneously formed during isothermal crystallization. This tendency faints with decreasing copolymer content. In blends with a majority of neat PEO, a single lamellar system is developed. The cocrystal systems are formed in all types of blends during crystallization. The LP1 lamellae in blends with PEO (3000) consist of extended chains of PEO (3000) and of extended PEO tails of copolymer. The LP1 cocrystal structures developed in blends with PEO (4000) are probably formed by NIF chains of PEO (4000) and NIF and EC of PEO tails of the copolymer. The LP2 lamellar systems are, in both kinds of blends, cocrystals consisting of 1F and NIF chains of both components. The PPO part of the copolymer predominantly forms amorphous interlayers of lamellae incorporating also chain ends and folds.

X-RAY DIFFRACTION ANALYSIS OF ETTRINGITE

V. Frank[1], A. Buchal[2] and J. Havlica[1]

[1] *Department of Material Chemistry, Faculty of Chemistry, Brno University of Technology, Purkynova 118, 612 00 Brno, Czech Republic*

[2] *Department of Material Engineering, Faculty of Mechanical Engineering, Brno University of Technology, Technicka 2, 616 69 Brno, Czech Republic*

Phase composition was determined by X–ray powder diffractometer. In first period of work, distilled water, aluminium sulphate (p. a.) and calcium oxide annealing from $CaCO_3$ were used as starting materials. In second step, drinking (industrial) water, ammonium aluminium sulphate from the production of chemical exploitation of uranium and technical burnt–lime were used. It was established that staring materials do not play important role in the product composition if their dosage is optimal. Differences were found in crystal morphology only.

Introduction

Ettringite $3 CaO . Al_2O_3 . 3 CaSO_4 . 32 H_2O$ is the prototype of the AFt phases of hydrated cement which have the general formula (tricalcium)–Aluminate Ferrite . tri (sulphate, hydroxide, etc.) . 32 (hydrate). Smolczyk first suggested the AFt designation in 1961 publication in order to distinguish the high sulphate hydrate phases from the low sulphate phases, which are collectively termed AFm (Aluminate Ferrite . mono) [1]. Ettringite occurs as a natural mineral along with others of similar structure and com-

positions fitting into the ettringite group of minerals. The crystal structure of ettringite was described by Moore and Taylor [2].

The aim of the presented work is:
• preparation of ettringite from pure chemicals (distilled water, CaO or $Ca(OH)_2$ and $Al_2(SO)_4$ with an analytical purity)
• preparation of ettringite from secondary raw materials like ammonium aluminium sulphate from the production of chemical exploitation of uranium and commercially produced lime
• determination of dependence of sample structure on starting materials and used water by X–ray analysis method
• characterisation of morphology of prepared samples

Experimental

Primarily the ettringite from suspension of $Ca(OH)_2$ and solutions of aluminium sulphate (p.a.Lachema, Brno) with mass concentration 40 g/l, then 80 and 160 g/l was prepared.

In the second step, the formation of ettringite was realised from solutions of technical ammonium aluminium sulphate (alum, produced by DIAMO enterprise, Strá□ pod Ralskem). Mass concentrations of the alum in water were 40, 80 and 130 g/l, where the last concentration represents saturated solution. In the table 4 result of ICP–OES analysis of alum solution is shown.

The apparatus has consisted of automatic burette with a solution of aluminium sulphate or ammonium aluminium sulphate, beaker with $Ca(OH)_2$ suspension, magnetic stirrer and pH meter – Precision Digital pH meter OP–208/1 Radelkis with two electrodes (glass and reference saturated calomel). At last period of ettringite preparation, an aluminium sulphate or ammonium aluminium sulphate solution was dropped from an automatic burette. During experiment, pH value was measured. Titration of solution was finished at pH = 10,7.
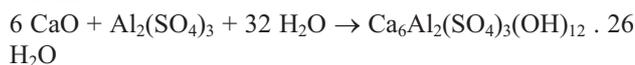
Finally an ettringite suspension was by low-pressure filtration processed and placed into a desiccator.

Phase analysis of samples was made by automated X–ray diffractometer X'Pert with central focusing configuration (Bragg–Brentano) in θ/θ implementation produced by firm PHILIPS (in 1999 Almelo, Netherlands). The diffractometer X'Pert had a Cu target X–ray tube completed with a Göbel mirror for parallel beam. The system was controlled by an automatic personal computer DELL. The control PC for evaluation of results contained a powder database PDF3 (ICDD–JCPDS) and a structure database ICSD. Morphology of samples was by scanning electron microscope PHILIPS XL30 detected.

Results and discussion

Presented work shows that ettringite formation is possible without sucrose improving transport of ions through solution by increasing of Ca^{2+} ions concentration as was reviewed in [3]. It was demonstrated, the ettringite crystals preparation is significantly influenced by proportionality of adding of individual compounds into reaction water system. Pure ettringite phase can be prepared from large scale of water purity (distilled, drinking, industrial).

Generally ettringite formation can be described by the scheme:
$$6\ CaO + Al_2(SO_4)_3 + 32\ H_2O \rightarrow Ca_6Al_2(SO_4)_3(OH)_{12} \cdot 26\ H_2O$$
Besides this reaction, four types of local simultaneous reactions may play role in kinetics of crystallisation process, morphology and properties of products:

1. $Ca^{2+} + SO_4^{2-} \rightarrow CaSO_4 \qquad CaSO_4 + Al(OH)_4^- \rightarrow$ ettr.
The both reactions run, when stoichiometric ratio of starting materials (lime and aluminium sulphate or ammonium aluminium sulphate) is retained. In this only pure ettringite is present as is shown in Fig. 1 and 2. Fig. 1 represents sample prepared from solution of aluminium sulphate and Fig. 2 ammonium aluminium sulphate respectively. Comparison both results documents no difference in reaction mechanism.

Ettringite creates good developed needle and pillar crystals with length about 1 μm and width 0,1 μm. Samples prepared from aluminium sulphate and ammonium aluminium sulphate are characterised by different morphology. Distribution of particle size in last said figures is more regular. It is probably caused by:
• different ratio of $Al(OH)_4^-$ and SO_4^{2-} ions in initial materials
• pH value controlled by presence of Ca^{2+}/NH_4^+ ions
• NH_4^+ volume influenced nucleation and crystallisation of ettringite
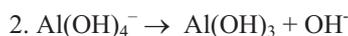
2. $Al(OH)_4^- \rightarrow Al(OH)_3 + OH^-$
This reaction manifests the non-stationary reaction condition. Local deficit of SO_4^{2-} ions in concentration gradient causes nucleation of metastable amorphous gibbsite $Al(OH)_3$. Precipitated alumina gel can block temporarily ettringite nucleation by reducing of $Al(OH)_4^-$ ions in solution. Alumina gel formation is manifested by higher background in X–ray pattern in Fig. 3.

Presence of portlandite $Ca(OH)_2$ is interesting with respect to deficit of Ca^{2+} ions. This fact can be explained by fast formation of alumina gel and by high activation energy of gibbsite dissolution. Beside these phases may crystallise gypsum $CaSO_4 \cdot 2\ H_2O$ too. It is caused by no stoichiometric ratio of input compounds.

In the first period of reaction, ettringite cannot form because all negligible compounds for building of crystal structure are not present in surround of possible nucleus. Only $Al(OH)_3$ and $CaSO_4 \cdot 2H_2O$ create.
In the second period, a part of soluble $CaSO_4 \cdot 2H_2O$ reacts with sulphates to ettringite. Insoluble alumina gel or gibbsite does not take part crystallisation. In final account, the deficit of aluminate ions causes presence of $Ca(OH)_2$ in phase composition of product. It can be concluded that low solubility of aluminate gel is a kinetic barrier for ettringite crystallisation.

3. $Ca^{2+} + 2\ OH^- \rightarrow Ca(OH)_2$
The reaction describes the situation with excess of Ca^{2+} ions in solution. Resultant solid phase composition is shown in Fig. 4. In the solid products are portlandite $Ca(OH)_2$ and ettringite. Last disposes all SO_4^{2-} and $Al(OH)_4^-$ ions. Higher content of Ca^{2+} ions increases pH
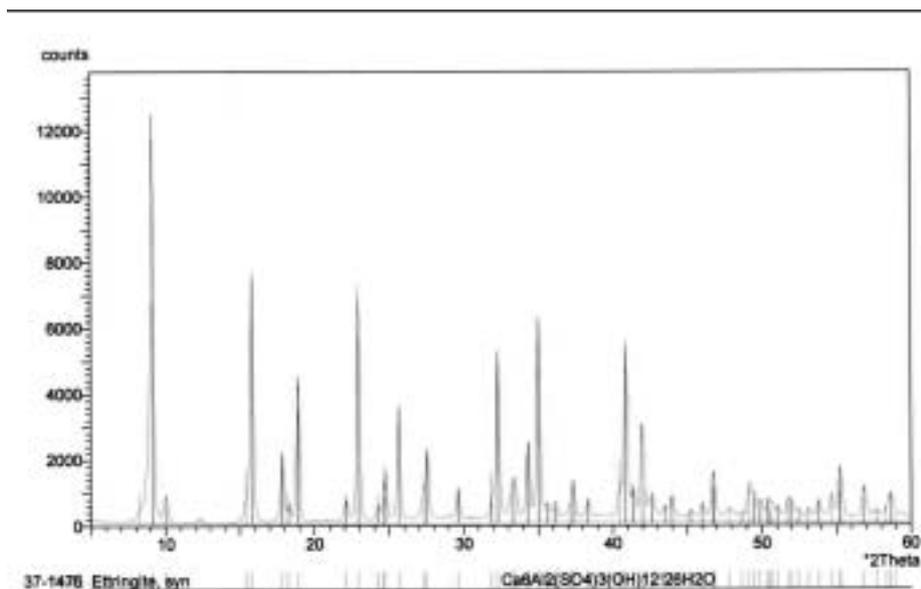
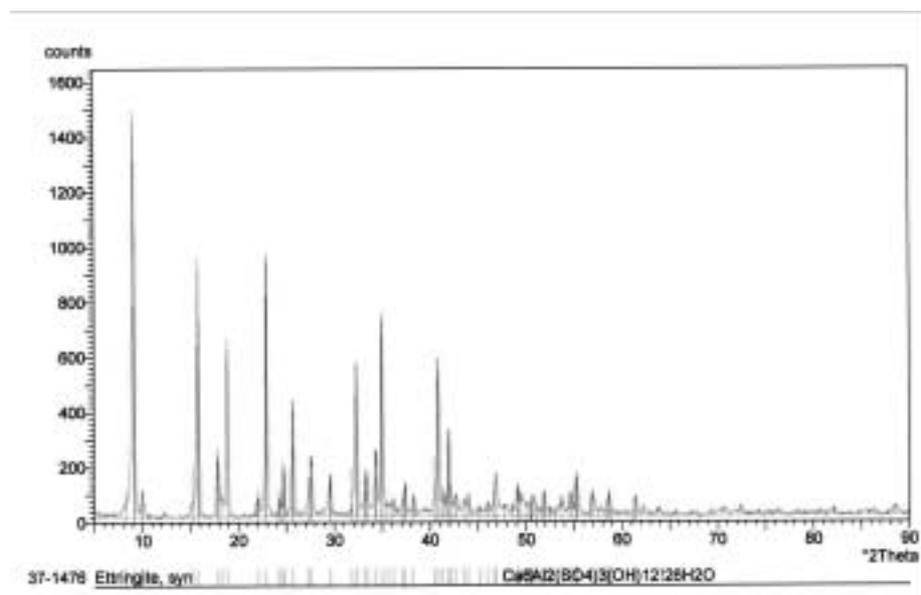**Figure. 1**. X–ray pattern with ettringite prepared from aluminium sulphate solution

Figure 2. X–ray pattern with ettringite prepared from ammonium aluminium sulphate
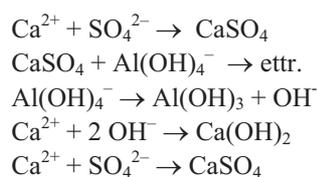
value and contributes to better transport of $Al(OH)_4^-$ ions in liquid phase. This fact leads to increasing of ettringite formation rate and reduction of gypsum precipitation probability X-ray pattern in Fig 4 is characterised by relative high ratio of amorphous phase.

4. $Ca^{2+} + SO_4^{2-} \rightarrow CaSO_4$
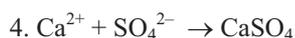
Local excess of SO_4^{2-} ions in solution causes gypsum crystallisation (Fig. 5) These conditions may be expected in technological plants with high rate of flow and that is why part of Al^{3+} is not effectively exploited for ettringite production. Fig. 18: System with precipitated gypsum beside ettringite

Conclusions

- The preparation of ettringite was realised from solutions of pure aluminium sulphate and technical ammonium aluminium sulphate.
- The apparatus for sample preparation was developed.
- On the basis of big number of samples, ettringite preparation was optimised.
- The ettringite crystals preparation is significantly influenced by proportionality of adding of individual compounds into reaction water system.
- Pure ettringite phase can be prepared from large scale of water purity (distilled, drinking, industrial).
- Beside main general reaction, four types of local simultaneous reactions may play role in kinetics of crystallisation process, morphology and properties of products:

$$Ca^{2+} + SO_4{}^{2-} \rightarrow CaSO_4$$
$$CaSO_4 + Al(OH)_4{}^- \rightarrow ettr.$$
$$Al(OH)_4{}^- \rightarrow Al(OH)_3 + OH^-$$
$$Ca^{2+} + 2\,OH^- \rightarrow Ca(OH)_2$$
$$Ca^{2+} + SO_4{}^{2-} \rightarrow CaSO_4$$

References:

1. Henderson, E. – Turrillas, X. – Barnes, P. In *J. Mat. Sci.* **30** (1995), p. 3856 - 3862.

2. Moore, A. E. – Taylor, H. F. W. Crystal Structure of Ettringite. In *Acta Crystallogr.* **B26** (1970), p. 386 - 393.

3. Struble, L. J. Synthesis and Characterization of Ettringite and Related Phases. *In* 8th International Congress on the Chemistry of Cement, 1987 p. 582-588 (vol. IV.)
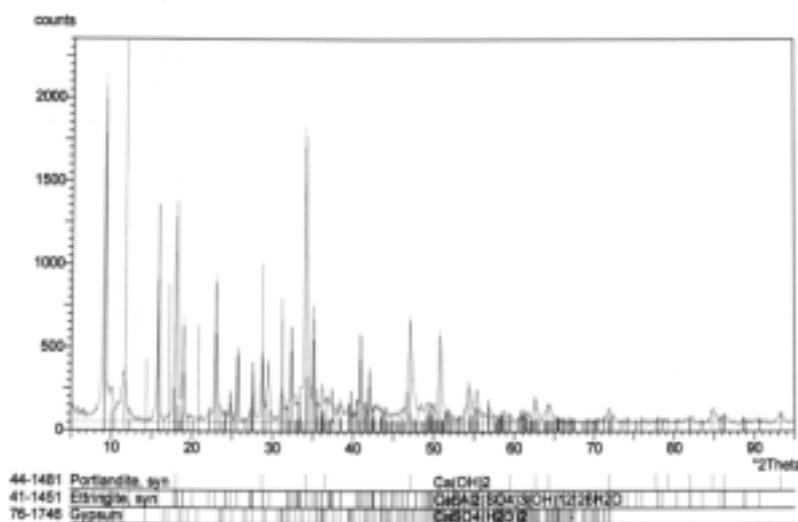
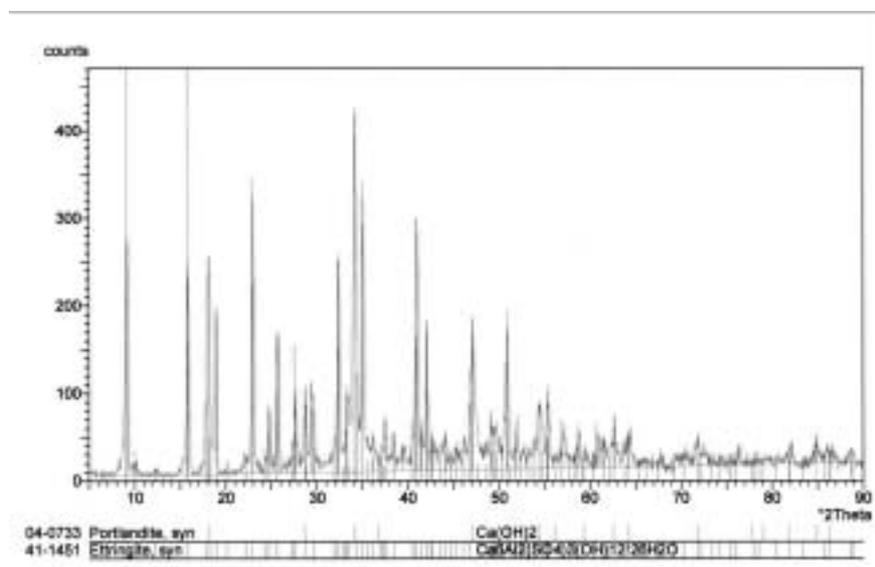**Figure 3**. X–ray pattern with higher background caused by alumina gel formation

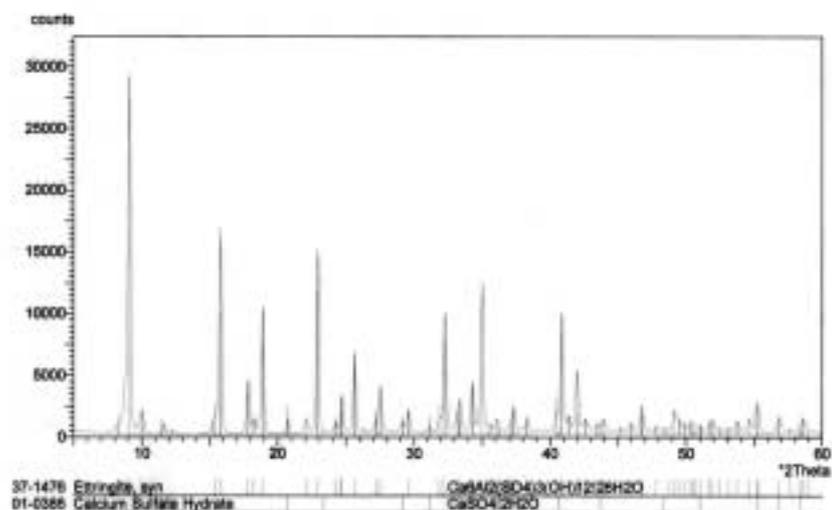**Figure 4**. X–ray pattern representing phase composition with Ca^{2+} ions in solution

Figure 5. System with precipitated gypsum beside ettringite